Xenon irradiation of Ni_3N/Si bilayers: Surface roughening and interface mixing and reactions

Leena Rissanen, Sankar Dhar, and Klaus-Peter Lieb*
II. Physikalisches Institut and Sonderforschungsbereich 345, Universität Göttingen, Bunsenstrasse 7-9, D-37073 Göttingen, Germany
(Received 7 April 2000; revised manuscript received 2 November 2000; published 28 March 2001)

The irradiation effects in Ni_3N/Si bilayers induced by 100–700 keV Xe ions at fluences up to 4×10^{16} ions/cm^2 were investigated at 80 K and room temperature. The element depth profiles were measured via Rutherford backscattering (Ni,Si) and resonant nuclear reaction (N) analysis, the phase formation at the interface via x-ray diffraction, and the surface roughness by atomic force microscopy. The observed dissociation and preferential sputtering of Ni_3N followed by nitrogen out-diffusion were related to the small binding energy of this compound. Mixing at the Ni_3N/Si interface occurs via a combination of diffusion and reaction controlled transport processes and the interface broadening varies in second order with the ion fluence. At higher ion fluences, the formation of $NiSi_2$ and Si_3N_4 phases at the interface was found.

DOI: 10.1103/PhysRevB.63.155411 PACS number(s): 68.55.Ln, 61.80.−x, 73.40.−c, 61.85.+p

I. INTRODUCTION

Irradiation of materials with ion beams having energies of a few hundred keV can improve the optical, chemical, tribological and electrical properties.[1,2] The ion-beam technique, in various forms, has been applied to semiconductors, metals, ceramics, polymers, and glasses in producing stable, metastable, or even non-equilibrium phases. Ion beam mixing[3–10] in elemental metal/metal and metal/semiconductor bilayer and multilayer systems has been investigated in a rather comprehensive way, in order to understand the ion-induced atomic transport processes and the formation of intermetallic phases at the interface(s). The relative importance of various mixing mechanisms, such as ballistic mixing, thermal spike mixing, and radiation-enhanced diffusion, has been established.[3–8] The transitions between these various scenarios concerning the ion parameters (mass, energy, and fluence) and thermodynamic properties and temperature of the samples are still being debated. Usually, ''athermal'' mixing via thermal spikes is expected to set in above the critical average element number $Z_{ave}=20$ of the target.[3,7] In the transition region around $Z_{ave}=20$ the atomic transport process changes from purely ballistic transport,[8] where the athermal mixing is due to collision cascades, to thermal spikes, where chemical forces enhance the atomic transport rates.[3–7] For example, using Xe ion beam, Ni/AlN ($Z_{ave}=11.5$) bilayers[11] exhibit ballistic atomic transport and therefore low mixing rates, while in Ni/Al ($Z_{ave}=20.5$) bilayers,[12] thermal spikes are induced leading to high mixing rates. The irradiation of Ni/Si ($Z_{ave}=21$) bilayers[4] finally leads to the formation of nickel silicide phases. Recently,[4,5] it has also been found that the formation of compounds increases the atomic mobility across the interface.

Technically, it appears more important to study the ion beam irradiation effects in ceramic/metal or ceramic/semiconductor systems, involving carbides, nitrides, or oxides, than in the metal/metal bilayers. Our rather systematic investigations on nitride/metal ($Z_{ave}=10-20$) bilayers[3,11] involving CrN, Cr_2N, AlN, and TiN nitride films on various metal substrates and irradiated by heavy noble gas ions (Ar, Kr, and Xe) led to rather small mixing rates and the conclusion that ballistic mixing prevails. Neither ion-beam induced dissociation of the nitride film nor enhanced nitrogen diffusion across the interface or nitride formation with the metal film was observed. This finding was related to the high binding energies of the nitrides studied. The only exception was found in Ni_3N/Al[13] bilayers ($Z_{ave}=18$) in which larger than ballistic mixing rates were observed and associated with the relatively weak binding of this compound. This result motivated us to study heavy ion irradiation effects in the ceramic/semiconductor system Ni_3N/Si ($Z_{ave}=18.3$). The preliminary results reported in Ref. 14 exhibit interesting new features of non-linear interface broadening and chemical reactions. In this paper, we present detailed results on the ion beam induced modifications of the surface and the interface region of Ni_3N/Si bilayers at different ion energies and irradiation temperatures. These results clearly demonstrate the role of thermochemical properties on the transport process and the phase formation at the bilayer interface in such a low Z system.

II. SAMPLE PREPARATION, IRRADIATION CONDITIONS, AND ANALYZING METHODS

The 70–250 nm thick nickel nitride films were deposited on HF-cleaned Si⟨100⟩ substrates via magnetron sputtering, using a permanent-magnet planar-type RF magnetron from Iontech, Ltd.[15] The system employed a 500 W RF-generator, and during the deposition the power of 150 W was used. The base pressure of the vacuum chamber was about 10^{-4} Pa and the working pressure was 0.5 Pa. The sputtering target was a high-purity nickel disc (99.999% Ni) with a diameter of 76 mm and a thickness of 6 mm. The deposition was performed in an atmosphere of pure argon and nitrogen gas flow, adjusted by two independent mass-flow controllers (max. flow 30 standard cubic centimeters). The substrate temperature was kept at 383 K. The deposition rate was ~0.4 nm/min. The ion irradiations were performed with 100–700 keV Xe^+ ions at fluences of $(0.5-4.0)\times10^{16}$ ions/cm^2 using the Göttingen heavy ion implanter IONAS.[16,17] The projected ion

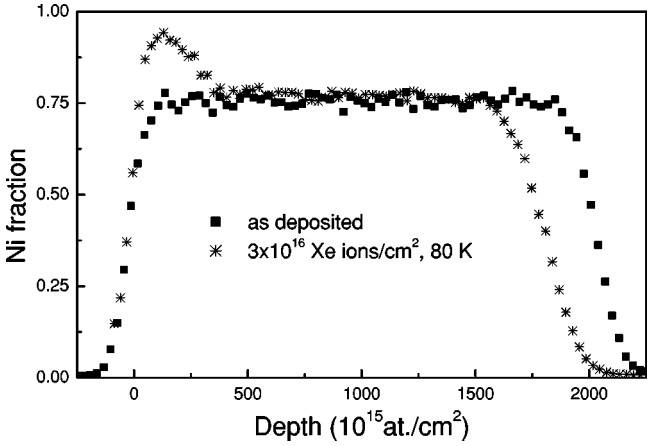

FIG. 1. Ni profile obtained from RBS analysis of an as-deposited Ni_3N film and a sample irradiated with 3×10^{16} Xe-ions/cm^2 at 450 keV and 80 K.

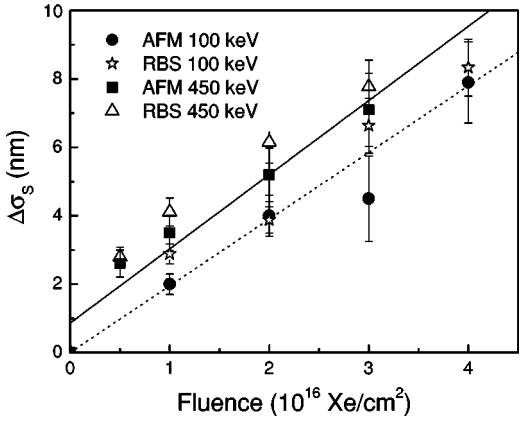

FIG. 2. Increased surface roughness $\Delta\sigma_S$ of samples irradiated at 80 K with 100 and 450 keV Xe ions and analyzed at room temperature both with RBS and AFM.

ranges were calculated with the TRIM95 program.[18] During the irradiation, the samples were either cooled to 80 K or kept at room temperature (RT). The ion flux was maintained at about 0.7 particle μA/cm^2 in order to avoid beam heating. Using a XY beam sweeping system, homogeneous implantations were achieved over an area of 10×10 mm^2.

The composition and thickness of the thin films were determined by Rutherford backscattering spectrometry (RBS) using 900 keV α-particles from IONAS.[16] The backscattered α-particles were registered at an angle of 165° relative to the beam by means of two Si surface detectors with about 14 keV energy resolution. The RBS spectra were analyzed with the RUMP program.[19] Since in the mixing experiments the Ni and Xe signals overlap in the RBS spectra, the spectra had to be deconvoluted. The Xe implantation profile was simulated by means of TRIM95 and included into the deconvolution via an asymmetric Gaussian distribution. Accurate nitrogen depth profiles were obtained from resonant nuclear reaction analysis (RNRA) using the $^{15}N(p,\alpha\gamma)^{12}C$ reaction at the 429.6 keV resonance energy, having the resonance width of $\Gamma=124$ eV.[20] During the RNRA measurements, the samples were cooled to 80 K in order to avoid any damage or further annealing due to the proton beam. The crystalline structure of the films was identified by x-ray diffraction (XRD), using a BRUKER AXS type D8 spectrometer with a copper anode at a fixed incidence angle of $\theta=5°$. The surface topography, especially the mean roughness, was determined by atomic force microscopy (AFM) using a Nanoscope II of DIGITAL INSTRUMENTS in tapping mode.

III. IRRADIATION EFFECTS ON Ni_3N LAYERS

In order to investigate the changes in composition and surface roughness due to irradiation, the Ni_3N films were bombarded with 450 and 100 keV Xe^+ ions at 80 K. The projected range of 450 keV Xe ions in Ni_3N is about 75 nm and that of 100 keV ions about 25 nm. The film thickness was chosen so that all the ions were stopped in the nitride film and did not reach the silicon substrate. Figure 1 presents the Ni-profile of an as-deposited 210 nm thick sample together with the profile obtained after irradiating this sample at 450 keV and a fluence of 3×10^{16} ions/cm^2, as obtained by RBS. The main visible features are (1) the reduction of the Ni_3N film thickness due to sputtering; (2) the increase of the Ni content in the near-surface region of the remaining Ni_3N film due to the loss of nitrogen (preferential sputtering); and (3) a slight broadening of the back-edge signal of the Ni profile due to the increased surface roughness. Note that all the implanted Xe ions are embedded in Ni_3N layer and do not cause any atomic transport through the Ni_3N/Si interface. Similar effects were observed for the case of 100 keV irradiation. The loss of nitrogen was independently determined by RNRA analysis. The sputtering rate at both energies was about 6–7 atoms per Xe ion. As to the preferential sputtering, i.e., the dissociation of Ni_3N and loss of nitrogen, we found that in a 20–25 nm surface layer the nitrogen content was reduced up to 20% under ion bombardments. This corresponds to the increase of the Ni content in Fig. 1. The thickness of the N-depleted zone was about constant, while the sputtered layer (as seen by the overall thickness of Ni_3N) increased proportionally to the fluence.

The broadening at the back edge of the Ni profile can be used for determining the surface roughening due to irradiation. The surface roughness measured by RBS analysis was independently determined by AFM for both energies. The linear roughness increase obtained by both methods, $\Delta\sigma_S(\Phi)=\sigma_S(\Phi)-\sigma_S(0)$, is plotted in Fig. 2 as a function of the ion fluence Φ. The quantity $\sigma_S(0)=(\sigma_S^2(0))^{1/2}$, where $\sigma_S^2(0)$ denotes the variance of the surface roughness in the as-deposited Ni_3N film, was obtained either from RBS and AFM. At both ion energies, $\Delta\sigma_S(\Phi)$ was found to grow linearly with Φ. Using the density of Ni_3N, 97.13 atoms/nm^3, the Xe ions induce an increase of the roughness by $\Delta\sigma_S\approx2$ nm per 1×10^{16} ions/cm^2.

IV. IRRADIATION EFFECTS AT THE Ni_3N/Si INTERFACE

In order to study the ion-beam induced effects at the Ni_3N/Si interface, the 75 ± 6 nm Ni_3N on Si samples were irradiated with 450 and 700 keV Xe ions at room temperature or at 80 K. The thickness of the films was chosen in

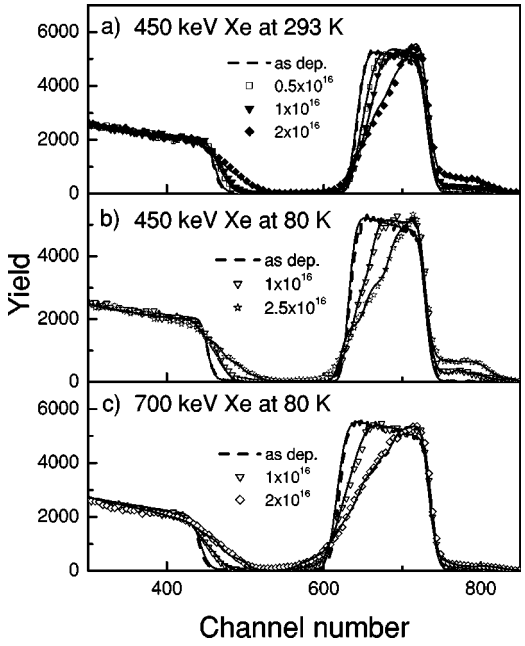

FIG. 3. RBS spectra of samples irradiated with (a) 450 keV Xe ions at room temperature, (b) 450 keV Xe ions at 80 K, and (c) 700 keV Xe ions at 80 K.

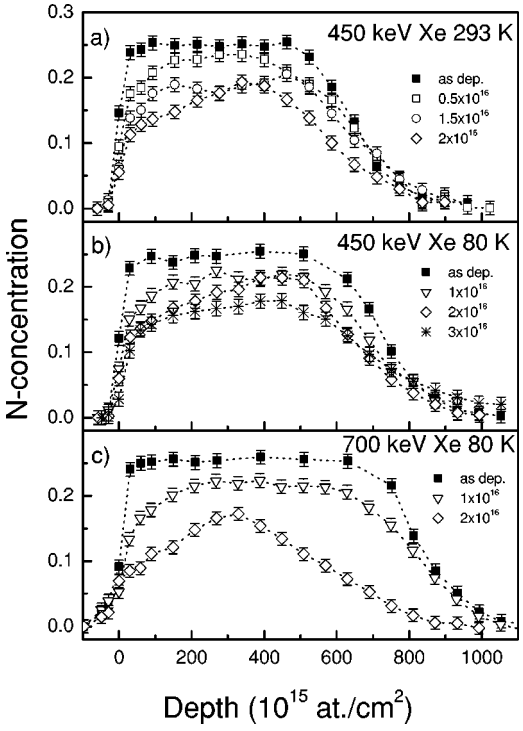

FIG. 4. RNRA nitrogen profiles of samples irradiated with (a) 450 keV Xe ions at room temperature, (b) 450 keV Xe ions at 80 K, and (c) 700 keV Xe ions at 80 K.

such a way that almost all ions would reach the silicon substrate. Since the correct density at the interface after irradiation is not known, the depth scale is given in units of 10^{15} atoms/cm^2. Then, the average density (73.56 atoms/nm^3) of Ni_3N/Si was used to convert it to the nm scale. For describing the interface broadening variance, $\Delta\sigma^2_{\mathrm{Int}}(\Phi)$, deduced from the RBS analyses, it is essential to know the connection between the irradiation parameters (fluence and energy) and the surface roughness. We used the expression $\Delta\sigma^2_{\mathrm{Int}}(\Phi) = \Delta\sigma^2_{\mathrm{RBS}}(\Phi) - \Delta\sigma^2_{S}(\Phi)$, which corrects the variance of the element profiles at the interface determined from RBS, $\Delta\sigma^2_{\mathrm{RBS}}(\Phi)$, with respect to the increase of the surface roughness, $\Delta\sigma^2_{S}(\Phi)$, for which we used the values obtained at 450 keV beam energy (Fig. 2). From these values of $\Delta\sigma^2_{\mathrm{Int}}(\Phi)$, we then calculated the experimental interface broadening rates $\Delta\sigma^2_{\mathrm{Int}}(\Phi)/\Phi$, which will serve as the basis for comparison with theory. In all cases, the fluence dependence of the parameter $\Delta\sigma^2_{\mathrm{Int}}(\Phi)/\Phi$ was approximated by a linear function, $\Delta\sigma^2_{\mathrm{Int}}(\Phi)/\Phi = k + m\Phi$, where the coefficients k and m are constants.

A. 450 keV irradiations at room temperature

The RBS spectra of as-deposited and irradiated Ni_3N/Si samples (450 keV, RT, $\Phi = 0.5$, 1 and 2×10^{16} ions/cm^2) are presented in Fig. 3(a). An increase in the interface broadening with increasing ion fluence is clearly seen in the spectra. The loss in the film thickness due to sputtering is obvious; a fluence of 1×10^{16} ions/cm^2 removes 10–15 nm of the nitride film. The accumulation of the Xe content with increasing fluence can also be followed. It grows with every irradiation step, but does not reach saturation. Again, the increased Ni yield of the RBS signal after irradiation indicates the dissociation of Ni_3N and preferred loss of nitrogen in the surface region. Figure 4(a) shows the RNRA nitrogen profiles in the as-deposited sample and in films irradiated with 0.5, 1.5, and 2×10^{16} ions/cm^2. For increasing fluence, the nitrogen content decreases, but not evenly throughout the whole layer, as the loss is more pronounced near the surface. This result was already observed in ion irradiations of Ni_3N/Al bilayers.[13] Thus the Ni yield near the surface increases mostly due to the out-diffusion of N. The interface broadening is also noticeable from the nitrogen profiles. The elemental (Ni and Si) profiles of the as-deposited and irradiated samples deduced from the RBS spectra are plotted in Fig. 5. Both profiles consistently show the changes of the film composition and the broadening of the interface due to the irradiations. The loss of nitrogen equals the gain of Ni in the surface region. At a fluence of 2×10^{16} ions/cm^2, the Si profile has reached the surface, thus drastically changing the relative elemental compositions.

B. 450 keV irradiations at 80 K

Interface broadening was also studied at 450 keV Xe ion energy and 80 K. At this temperature, radiation-enhanced diffusion is expected to be suppressed. In Fig. 3(b), the RBS spectra of the samples irradiated with fluences of 1, 2, and 2.5×10^{16} ions/cm^2 are presented. The spectra are very similar to the ones taken at room temperature, but the Ni yield of the spectra does not increase as much with the increasing fluence as at RT. This could partly result from the deconvolution of the overlapping Xe and Ni peaks. Therefore, it is more convenient to look at the nitrogen concentration pro-

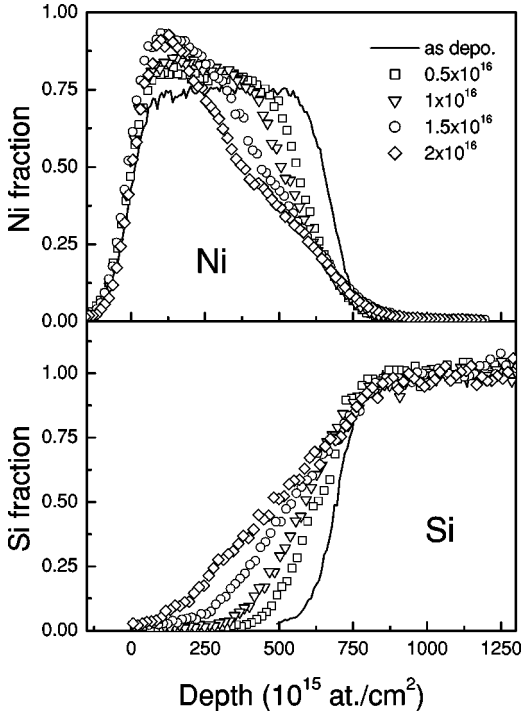

FIG. 5. Elemental profiles of Ni_3N/Si films irradiated with 450 keV Xe ions at room temperature.

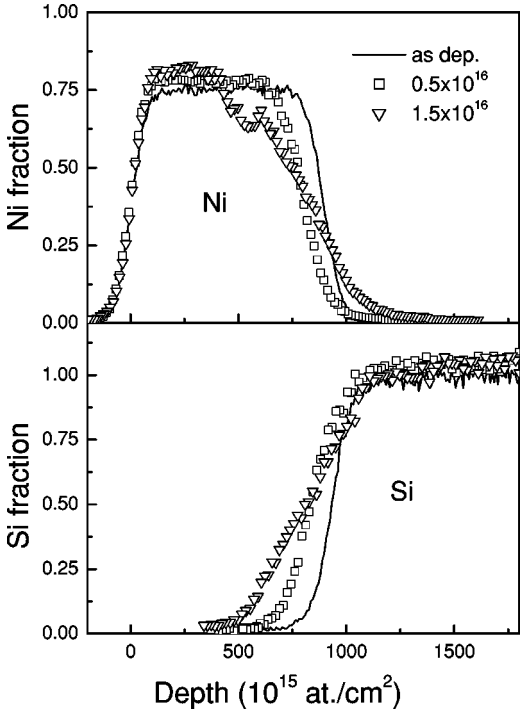

FIG. 6. Elemental profiles of Ni_3N/Si films before and after irradiation with 700 keV Xe ions at 80 K.

files obtained via RNRA [see Fig. 4(b)]. Indeed, the loss of nitrogen near the surface is slightly weaker than at room temperature, but again increases with the ion fluence. The lower temperature obviously suppresses the out-diffusion of nitrogen to some extent. Otherwise, the trend of the profiles is similar at all fluences, the maximum nitrogen content is found in the interface region.

C. 700 keV irradiations at 80 K

Finally, the 80 K irradiations were repeated at 700 keV ion energy. The RBS spectra of these irradiations are displayed in Fig. 3(c). When compared to the results obtained at 450 keV and 80 and 293 K, the broadening of the interface region is similar. At 700 keV, the Xe signal strongly overlaps with the Ni signal and thus requires a very careful deconvolution of the RBS spectra. Under these circumstances, the independent determination of the nitrogen content via RNRA was mandatory to check the film composition. The elemental profiles (see Fig. 6) indeed show that the change in the nickel content at the surface region is smaller than in the 450 keV irradiations at 293 and 80 K. In Fig. 4(c) the nitrogen profiles determined by RNRA are plotted. Compared with the 450 keV irradiation, there are no differences up to 1×10^{16} ions/cm^2. At 2×10^{16} ions/cm^2 the shape of the nitrogen content differs from that of the others. First, more nitrogen has been lost than at 450 keV. Second, the maximum of the nitrogen peak has moved towards the surface.

D. Phase formation

In order to identify the formation of new phases induced by the Xe ion irradiation, XRD spectra were accumulated, some of which are presented in Fig. 7. The thickness of the as-deposited Ni_3N film was 80 nm. The XRD analysis of this sample shows that the Ni_3N film [see Fig. 7(a)] has a hexagonal crystal structure[21] with lattice constants of $a=0.462$ nm and $c=0.430$ nm. Figure 7(b) shows the XRD spectrum

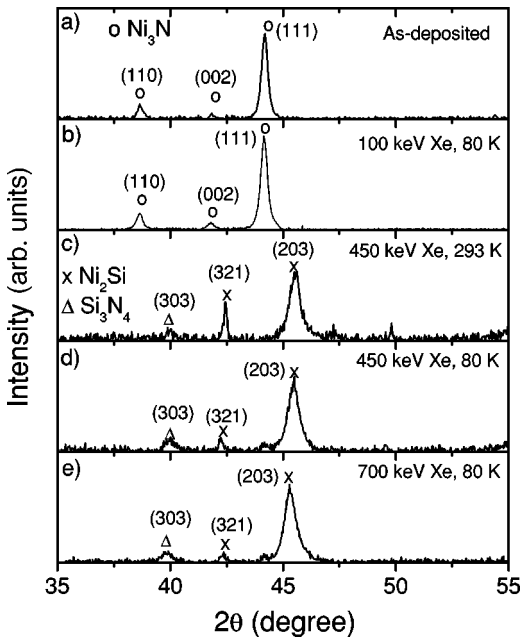

FIG. 7. XRD spectra of Ni_3N/Si bilayers taken (a) for an as-deposited sample; (b) after a Xe bombardment at 100 keV and 80 K; (c) after irradiation at 450 keV and room temperature; (d) at 450 keV and 80 K with (e) at 700 keV and 80 K. In all cases, (b)–(e), the Xe ion fluence was 1×10^{16} ions/cm^2.

taken after 100 keV Xe irradiations at 80 K. Even though some amount of nitrogen is lost from the surface region, the reflexes remain in the same positions, as in Fig. 1(a), but they are now slightly broadened. This is related to the reduction of the grain size. The decrease in grain size was also observed by AFM. It should be pointed out that the depth of the XRD analysis is much larger than the thickness of the nitride layer, where preferential sputtering occurs. At 450 and 700 keV, the ions penetrate the interface and new peaks emerge in the spectrum [Figs. 7(c)–7(e)]. They are belonging to Ni_2Si and Si_3N_4 phases, which are also expected to be energetically the most favored ones. The higher the irradiation energy, the sample temperature and the irradiation fluence, the stronger was the growth of these new phases.

V. DISCUSSION

A. Parametrization of the interface broadening rates

As we have seen in Sec. IV, the chosen combination of analyzing techniques provides detailed information on the atomic transport and phase formation processes in Ni_3N/Si bilayers irradiated by energetic Xe-ions. Summarizing the various effects, which occur at the surface of the Ni_3N film, we have been able to differentiate surface roughening, sputtering of Ni_3N film, and preferential loss of nitrogen from the near-surface layers. At the Ni_3N/Si interface, we find strong ion-beam mixing associated with the formation of Ni_2Si and Si_3N_4 phases. All the interface processes have been found at both 80 K and room temperatures, and whenever the Xe ion energy was sufficiently high to penetrate the Ni_3N/Si interface. The formation of both Ni_2Si and Si_3N_4 phases observed by XRD was most pronounced at 80 K with 700 keV Xe ions.

The deduced Ni and Si elemental profiles were used to determine the interface broadening rates, $\Delta\sigma^2_{\mathrm{Int}}=\Delta\sigma^2_{\mathrm{RBS}}-\Delta\sigma^2_S$, after the increase $\Delta\sigma^2_S$ of the surface roughness had been taken into account. In Fig. 8, the fits resulting in second-order polynomials are plotted as function of the fluence. The interface broadening rates $\Delta\sigma^2_{\mathrm{Int}}/\Phi$ were then fitted by the expression $\Delta\sigma^2_{\mathrm{Int}}/\Phi\ [\mathrm{nm}^4]=k+m\Phi$, where Φ is given in the unit of 10^{16} ions/cm$^2=10^2$ ions/nm^2. Table I summarizes the measured mixing parameters k and m found at the various irradiation conditions. The mixing parameters obtained at 450 keV, 80 K differ somewhat from the ones obtained at 700 keV, 80 K and 450 keV, 293 K. The two latter fits are very similar and feature a small value of $k\approx 0.3$ nm^4 and a large linear term, $m\approx 2.5$ nm$^4/10^{16}$ cm^{-2}, while the former case exhibits a larger value of $k\approx 1.4$ nm^4 and a smaller linear term, $m=1.8$ nm$^4/10^{16}$ cm^{-2}. In order to illustrate the constant and linear contributions to the mixing for each case, the interface broadening rates $\Delta\sigma^2_{\mathrm{Int}}/\Phi$ presented in nm^4 units are plotted versus the irradiation fluence Φ in Fig. 9. In spite of the difference mentioned before, it should be noted that the overall fluence dependence of $\Delta\sigma^2_{\mathrm{Int}}/\Phi$ is very similar in all three cases. It is important to mention that these experimentally obtained quantities (i.e., k and m) contain uncertainties that arise due to the use of the average atomic density of Ni_3N and Si for converting the depth unit into the nm scale, and also due to the variation of deposition energies. The exact density in the intermixed region is difficult to predict since the mixed region is a mixture of several phases. However, Fig. 8 clearly shows that the quadratic fluence dependence holds where the depth scale is independent of the atomic density. It may be noted that under similar irradiation conditions (450 keV Xe ion at 80 K) we observe a constant broadening rate on fluence in the Ni_3N/Al system.[22]

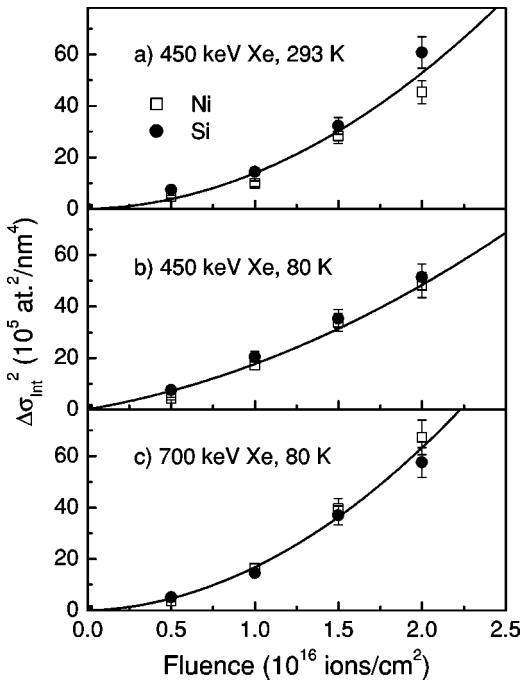

FIG. 8. Interface broadening variances $\Delta\sigma^2_{\mathrm{Int}}$ of samples irradiated with (a) 450 keV Xe ions at room temperature, (b) 450 keV Xe ions at 80 K, and (c) 700 keV Xe ions at 80 K. The solid lines are the fitted curves.

B. Diffusion versus reaction-controlled mixing

In the following, we try to interpret the interface broadening rates $\Delta\sigma^2_{\mathrm{Int}}/\Phi$ in terms of current models on ion beam mixing.[3–8] The occurrence of a constant and linear contribution to the mixing rates may be explained in the following way:[4] a constant mixing rate usually points to a diffusion-controlled process; the linear dependence, on the other hand, refers to a process governed by a chemical reaction rate. In some metal/silicon bilayer systems forming silicides under ion irradiation, such as Pd/Si, the fluence ranges, over which the individual processes dominate, are clearly divided.[4] Below a critical fluence Φ_c, the atomic transport process is reaction-controlled (linear mixing rate), and above that fluence it becomes diffusion-controlled (constant mixing rate). On the other hand, the interface broadening rates of ion-irradiated Ni/Si and Cr/Si bilayers were found to be either constant or linearly dependent on Φ, respectively. In all these cases silicides are formed. The reaction rate (speed) R determines the value of the critical fluence Φ_c: in the Ni/Si system the small upper limit of $\Phi_c \ll 1.5\times 10^{14}$ Au ions/cm^2

TABLE I. Experimental and theoretical interface broadening rates $\Delta\sigma_{int}^2/\Phi$ of Xe-ion irradiated Ni_3N/Si bilayers, obtained at the ion energies and substrate temperatures indicated. The coefficients k and m are defined via $\Delta\sigma_{int}^2/\Phi = k + m\Phi$. For the theoretical numbers k_{ball} and k_{comp}, see text.

Xe ion energy (keV)	T (K)	Experimental rate coefficients k (nm^4), m (nm^4/10^{16} cm^{-2})	Ballistic model k_{ball} (nm^4)	Compound formation model k_{comp} (nm^4)	Phase formation
450	80	1.4±0.2, 1.8±0.2	0.20	1.6	Ni_2Si, Si_3N_4
700	80	0.38±0.10, 2.7±0.4	0.22	1.8	Ni_2Si, Si_3N_4
450	293	0.25±0.03, 2.3±0.3	0.20	1.6	Ni_2Si, Si_3N_4

leads to a very high reaction rate ($R \gg 1$ nm/s), while in the Pd/Si system the critical fluence of $\Phi_c = 1.5\times10^{15}$ Au ions/cm^2 leads to $R = 0.87$ nm/s. In the case of the Cr/Si system, the very high critical fluence of $\Phi_c = 1\times10^{19}$ Cr ions/cm^2 implies a very small reaction rate of $R = 1.2\times10^{-2}$ nm/s. These numbers indicate that, depending on the reaction rate R and the implanted fluence Φ, the interface broadening rate changes from a purely linear to a constant rate. Evidently, in the present case of Ni_3N/Si bilayers under Xe bombardment, these two processes occur simultaneously, probably due to the formation of two phases with different reaction rates. Such a behavior, especially in a bilayer system with $Z < 20$, is not yet clearly understood. Moreover, the dissociation of Ni_3N under ion irradiation, the (possibly radiation-enhanced) diffusion of N, Ni, and Si across the interface, and the chemical reactions going on to recombine these species is a very complex process.

C. Ballistic mixing

Several models[3–8] have been developed to explain the diffusion and reaction-controlled atomic transport processes (and phase formation) of binary systems under ion irradiation. As an energetic ion beam travels through the material, it loses energy by electronic and nuclear stopping and creates collisions cascades, whenever the target atoms receive sufficient energy to overcome the displacement energy. At a low displacement density, the atomic transport process, which is the predominant process in bilayers with $Z_{ave} \leqslant 20$, can be described by considering ballistic properties[8] of the materials that neglect the effect of chemical forces. In many nitride/metal bilayer systems,[3] the ballistic approach was found to give a good description of the mixing. According to Sigmund and Gras-Marti, the mixing rate[8] is then given by

$$k_{ball} = \Delta\sigma_{int}^2/\Phi = \frac{1}{6}\Gamma_0 \xi \frac{F_D R_d^2}{N E_d}, \tag{1}$$

where $\Gamma_0 = 0.608$ is a dimensionless constant; ξ a kinematic factor involving the masses of the colliding atoms; F_D the deposited energy density per ion and unit length; E_d the displacement energy; and N the average atomic density. (Evidently, this expression does not depend on the ion fluence, and thus cannot explain the observed linear part of the mixing rate.) The separation distance of a Frenkel pair, R_d, was approximated[3] to 1 nm and the corresponding displacement energy E_d to 20 eV/at. One of the crucial parameters in the ion-beam mixing models is the energy density F_D per ion deposited at the interface. Figure 10 presents F_D values as a function of the depth within the Ni_3N/Si film for 450 and 700 keV Xe ions, calculated with the program TRIM95.[18] During the 450 keV irradiation, F_D changes its value from about 2 keV/nm to 4 keV/nm, as the film thickness decreases due to the sputtering effect. For 700 keV ions the deposited energy has almost a constant value of 3.4 keV/nm, but starts to decrease at fluences above 3×10^{16} ions/cm^2, when the ni-

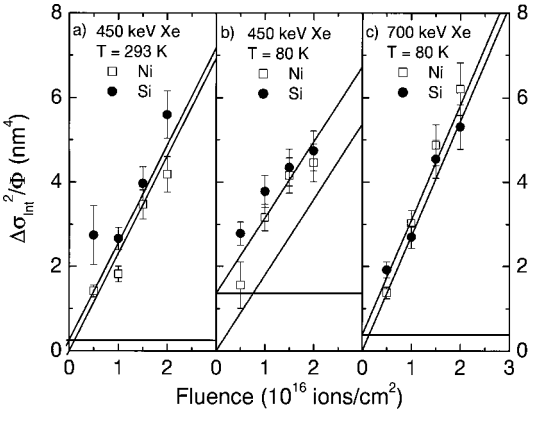

FIG. 9. Interface broadening rates $\Delta\sigma_{int}^2/\Phi$ of Ni_3N/Si bilayer samples as a function of the Xe-ion fluence Φ, at (a) 450 keV and room temperature, (b) 450 keV and 80 K, and (c) 700 keV and 80 K.

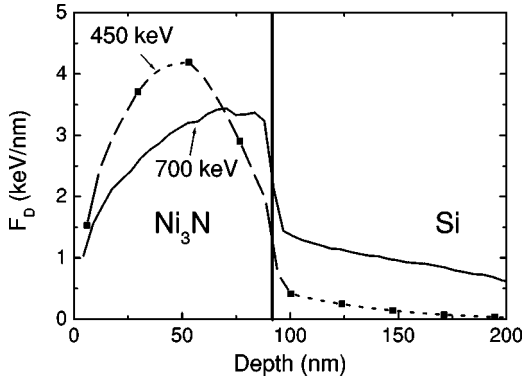

FIG. 10. The deposited energy density F_D for 450 and 700 keV Xe ions penetrating a Ni_3N/Si bilayer is plotted as a function of the depth. The calculations were performed with the program TRIM95.

tride layer thickness is reduced to about 40 nm, as a consequence of sputtering. The calculated ballistic mixing rate for 450 keV ions given in Table I refers to a mean value of the deposited energy of 3.0 keV/nm. When comparing the constant parts of the experimental interface broadening rates with this estimate of the ballistic model, we notice fair agreement for the 700 keV, 80 K and 450 keV, 293 K irradiations to within a factor of 2. Clearly, the large constant term found after the 450 keV, 80 K Xe irradiation is largely underestimated by the ballistic model.

D. Compound formation enhanced mixing

As pointed out, the XRD measurements revealed the formation of Ni_2Si and Si_3N_4 phases to take place at the interface and, interestingly enough, the nickel silicide was formed at a smaller fluence before the Si_3N_4 phase appeared. When either the irradiation temperature or the ion energy was increased, the Si_3N_4 phase appeared and the interface broadening rate turned out to be more reaction controlled. Recently, Desimoni and Traverse[4] have developed a formalism to account for the enhancement of the interface broadening rate due to the chemical reaction $A+C \rightarrow A_aC_c$ in an ion-beam irradiated A/C binary system ($Z_{ave}>20$). Unlike in the purely ballistic model, this approach[4,5] predicts a constant, as well as a linear, contribution of the mixing rates. The calculation of the latter is possible if the reaction rate R is known. We have extended this model to the present ternary system where more than one phase is formed under ion irradiation. The enhancement factor due to compound formation was estimated by taking into account the reaction $A_aB_b + C \rightarrow A_dC_e + C_fB_g$ occurring in an A_aB_b/C bilayer in which all the three species, A, B, and C are mobile. The modified linear term of the ballistic mixing rate, k_{comp}, is obtained by multiplying the ballistic rate k_{ball} from Eq. (1) with the compound formation enhancement factor f_{comp}:

$$k_{comp} = k_{ball} \cdot f_{comp}, \tag{2}$$

where

$$f_{comp} = 2\left[\frac{[a/(a+b)]N_{A_aB_b}}{[d/(d+e)]N_{A_dC_e}} + \frac{N_C}{[e/(d+e)]N_{A_dC_e}} + \frac{[b/(a+b)]N_{A_aB_b}}{[g/(g+f)]N_{C_fB_g}} + \frac{N_C}{[f/(g+f)]N_{C_fB_g}}\right],$$

where N_{XxYy} is the atomic density of the compound X_xY_y. The formation of Ni_2Si and Si_3N_4 phases at the interface suggests that the most likely chemical reaction to take place is $4\ Ni_3N + 9\ Si \rightarrow 6\ Ni_2Si + Si_3N_4$. Assuming Ni and N to be the predominantly[4] mobile species, the calculated coefficients k_{comp} are given in Table I. As compared to experiment, the value of k_{comp} has the right order of magnitude in the case of the 450 keV, 80 K irradiation, but overestimates the experiments in the two other cases, which are closer to the purely ballistic approach. It should be noted that the above calculated quantities are valid within the range of the approximated values of the atomic density and deposition energies in the intermixed region. The approximation is necessary as the exact values of these two quantities are difficult to ascertain.

As to the linear term of $\Delta\sigma^2_{Int}/\Phi$ addressing the reaction-controlled process, the coefficient $m_{comp}{}^4$ can be written as

$$m_{comp}(\text{reaction controlled}) = [f_{comp} \cdot R/\dot{\Phi}]^2, \tag{3}$$

where f_{comp} denotes the compound formation factor introduced in Eq. (2) and $\dot{\Phi} = 1\times10^{13}$ ions/cm^{2}s the ion flux used in the present work. Unfortunately, we cannot estimate the linear part of the broadening rate, as the reaction rates R are not known. However, if we assume this approach to be valid, then from the slopes of $\Delta\sigma^2_{Int}/\Phi$ (see Fig. 9) we can estimate the value of R, which may provide information to reach a better understanding the underlying physical picture of the mixing, reaction, and growth processes. The estimated average value, $R \approx 0.18\times10^{-2}$ nm/s, is similarly small as the one reported in the Cr/Si+Cr-ion system (1.2×10^{-2} nm/s). As mentioned before, only the linear dependence of $\Delta\sigma^2_{Int}/\Phi$ via a reaction-controlled process has been established in this system.[4] Hence, in the present Ni_3N/Si+Xe case, the situation is different insofar as both reaction-controlled and diffusion-controlled processes are active at all fluences. Unlike in a binary system, the simultaneous occurrence of both processes is probably due to the early decomposition of the weakly bonded Ni_3N layers. Hence, one may argue that the three elements react almost freely (and probably at different reaction rates), resulting in the growth of an interface layer having a non-homogeneous distribution of Ni_2Si and Si_3N_4 phases. The present experimental results indicate that the chemical nature (i.e., reactivity) of the elements determines the interface broadening and growth rate. However, all these processes and their dependence on the ion and material parameters are not clearly understood yet. Evidently, the processes in ternary systems are even more complex than those in binary systems and therefore more experimental information; e.g., mixing studies of nitride/metal bilayers having a weakly and strongly bonded nitride, is required.

VI. SUMMARY

The detailed mixing studies of thin Ni_3N/Si bilayers presented in this work employed a favorable combination of ion beam analytical methods, scanning tunneling microscopy, and x-ray diffraction. The importance of the various irradiation effects near the surface, such as surface sputtering and roughening, nitride dissociation and nitrogen depletion, and transport and phase formation at the interface has been stressed. Although the system appears to be ideally suited for a straightforward RBS analysis, depth profiling of nitrogen (via RNRA), as well as phase and surface analyses, turned out to be essential for interpreting the RBS spectra and achieving realistic interface mixing rates. The thermochemical properties of the (ternary) system play an important role in understanding the irradiation-induced processes. The theory of ballistic mixing, which so far has been rather successful in most nitride/metal bilayer mixing experiments, was extended to accommodate diffusion and reaction-

controlled processes and to estimate the constant and linear terms in the interface broadening rates. The present approximation, which was originally developed for elemental systems where the mixing is governed by thermal spikes, was shown to work at least to some extent for a light three-element system. In contrast to most metal/semiconductor systems where the reaction and diffusion-controlled fluence ranges are clearly separated, in this particular ceramic/semiconductor system they do overlap, possibly as a result of the small binding energy of Ni_3N and the formation of Ni_2Si and Si_3N_4 phases at the interface. However, the rough estimates given may only serve as a first step to the understanding of the transport processes.

It should also be mentioned that the ion-induced growth at relatively low temperatures for highly reactive systems (i.e., silicides, aluminades, and germanides), should be viewed differently from those systems where a solid solution or amorphous phase is produced. In the latter case, long-range atomic migration or overcoming of the barrier to nucleation are necessary. However, for reactive systems where the diffusive flux of the reacting species is controlled by the reaction rate *R*, such barriers are either negligible or absent so that the system can undergo structural relaxation and produce stable equilibrium compounds. The role of ion irradiation is to supply the required flux of reacting species that participate in the compound formation at the reacting interface.

ACKNOWLEDGMENTS

The authors are indebted to Detlef Purschke for expertly running the IONAS accelerator and to Wolfgang Bolse for useful comments on the models used. This work was supported by Deutsche Forschungsgemeinschaft.

*Corresponding author; Email address: lieb@physik2.uni-goettingen.de

[1] A. Polman, J. Appl. Phys. **82**, 1 (1997).
[2] C. A. Straede, Nucl. Instrum. Methods Phys. Res. B **113**, 161 (1996).
[3] W. Bolse, Mater. Sci. Eng., R. **12**, 53 (1994); Mater. Sci. Eng., A **A253**, 194 (1998).
[4] J. Desimoni and A. Traverse, Phys. Rev. B **48**, 13 266 (1993).
[5] S. Dhar, Y. N. Mohapatra, and V. N. Kulkarni, Phys. Rev. B **54**, 5769 (1996).
[6] M. Nastasi and J. W. Mayer, Mater. Sci. Eng., R. **12**, 1 (1994).
[7] Y. T. Cheng, Mater. Sci. Rep. **5**, 45 (1990).
[8] P. Sigmund and A. Gras-Marti, Nucl. Instrum. Methods **182/183**, 25 (1981).
[9] G. S. Was, Prog. Surf. Sci. **32**, 211 (1990).
[10] B. X. Liu, Phys. Status Solidi A **94**, 11 (1986).
[11] T. Corts, A. Traverse, and W. Bolse, Nucl. Instrum. Methods Phys. Res. B **80/81**, 167 (1993).
[12] T. Weber and K. P. Lieb, J. Appl. Phys. **73**, 3499 (1993).
[13] M. Milosavljevic, T. Corts, K. P. Lieb, and N. Bibic, Nucl. Instrum. Methods Phys. Res. B **68**, 426 (1992).
[14] L. Rissanen, S. Dhar, K. P. Lieb, K. Engel, and M. Wenderoth, Nucl. Instrum. Methods Phys. Res. B **161-163**, 990 (2000).
[15] T. Kacsich, M. Niederdrenk, P. Schaaf, K. P. Lieb, U. Geyer, and O. Schulte, Surf. Coat. Technol. **93**, 32 (1997).
[16] K. P. Lieb, Contemp. Phys. **40**, 385 (1999).
[17] M. Uhrmacher, K. Pampus, F. J. Bergmeister, D. Purschke, and K. P. Lieb, Nucl. Instrum. Methods Phys. Res. B **9**, 234 (1985).
[18] J. F. Ziegeler, J. P. Biersack, and U. Littmark, *The Stopping and Range of Ions in Solids* (Pergamon Press, New York, 1985).
[19] R. L. Doolittle, Nucl. Instrum. Methods Phys. Res. B **15**, 227 (1986).
[20] Th. Osipowicz, K. P. Lieb, and S. Brüssermann, Nucl. Instrum. Methods Phys. Res. B **18**, 232 (1987).
[21] J. Sachze, Z. Anorg. Allg. Chem. **251**, 201 (1943).
[22] S. Dhar, L. Rissanen, K. P. Lieb, K. Engel, and M. Wenderoth, Nucl. Instrum. Methods Phys. Res. B (to be published).